

General Disclaimer

One or more of the Following Statements may affect this Document

- This document has been reproduced from the best copy furnished by the organizational source. It is being released in the interest of making available as much information as possible.
- This document may contain data, which exceeds the sheet parameters. It was furnished in this condition by the organizational source and is the best copy available.
- This document may contain tone-on-tone or color graphs, charts and/or pictures, which have been reproduced in black and white.
- This document is paginated as submitted by the original source.
- Portions of this document are not fully legible due to the historical nature of some of the material. However, it is the best reproduction available from the original submission.

"Made available under NASA sponsorship
in the interest of early and wide dis-
semination of Earth Resources Survey
Program information and without liability
for any use made thereof."



E83-10383

CR-172925

A PRELIMINARY EVALUATION OF LANDSAT-4 THEMATIC MAPPER DATA
FOR
THEIR GEOMETRIC AND RADIOMETRIC ACCURACIES

by

M.H. Podwysocki, L.U. Bender, N. Falcone and O. D. Jones
U.S. Geological Survey
Reston, Va. 22092

Original photography may be purchased
from EROS Data Center
Sioux Falls, SD 57199

(E83-10383) A PRELIMINARY EVALUATION OF
LANDSAT-4 THEMATIC MAPPER DATA FOR THEIR
GEOMETRIC AND RADIOMETRIC ACCURACIES
(Geological Survey) 18 p HC A02/MF A01

N83-32136

Unclass

CSCC USB G3/43 00383

ORIGINAL PAGE IS
OF POOR QUALITY

A PRELIMINARY EVALUATION OF LANDSAT-4 THEMATIC MAPPER DATA
FOR
THEIR GEOMETRIC AND RADIOMETRIC ACCURACIES

by

M.H. Podwysocki, L.U. Bender, N. Falcone and O. D. Jones
U.S. Geological Survey
Reston, Va. 22092

ABSTRACT

Some Landsat Thematic Mapper data collected over the eastern United States were analyzed for their whole-scene geometric accuracy, band-to-band registration and radiometric accuracy. Band-ratio images were created for a part of one scene in order to assess the capability of mapping geologic units with contrasting spectral properties. Systematic errors were found in the geometric accuracy of whole scenes, part of which were attributable to the film-writing device used to record the images to film. Band-to-band registration showed that bands 1 through 4 were registered to within one pixel. Likewise, bands 5 and 7 also were registered to within one pixel. However, bands 5 and 7 were misregistered with bands 1 through 4 by 1 to 2 pixels. Band 6 was misregistered by 4 pixels to bands 1 through 4. Radiometric analysis indicated two kinds of banding, a modulo-16 stripping and an alternate light-dark group of 16 scanlines. A color-ratio composite image consisting of TM band ratios $3/4$, $5/2$, and $5/7$ showed limonitic clay-rich soils, limonitic clay-poor soils, and nonlimonitic materials as distinctly different colors on the image.

ORIGINAL PAGE IS
OF POOR QUALITY

A PRELIMINARY EVALUATION OF LANDSAT-4 THEMATIC MAPPER DATA
FOR
THEIR GEOMETRIC AND RADIOMETRIC ACCURACIES

INTRODUCTION

This report describes results of some preliminary analyses of Landsat-4 Thematic Mapper data for the NASA Landsat Image Quality Analysis program (LIDQUA). The work is being done under interagency agreement S-12407-C between the U.S. Geological Survey and NASA-Goddard Space Flight Center (GSFC).

Landsat-4 TM scenes for Washington, D.C. (40109-15140, November 2, 1982) Macon, Georgia (40050-15333, September 4, 1982) and Cape Canaveral, Florida (40036-14214, August 20, 1982) have been examined to determine their geometric and radiometric accuracy. In addition, parts of these scenes are also being analyzed to determine the ability to identify specific rock types with the added near-infrared TM bands at 1.6 and 2.2 μm .

GEOMETRIC ANALYSIS

In order to assess whole scene geometric accuracy, each of the seven TM bands for the geometrically corrected (GSFC P-tape digital format) Washington, D.C. scene were contrast stretched and recorded on film using an Optronics P-1500 film writer. Thirty-eight well-defined control points (figs. 1a and b) were visually identified by comparing 1:24,000-scale topographic maps with TM band 3. Bender and Falcone¹ stated that the combined affect of map-position error (for maps meeting National Map Standards) and control-point identification error may yield a Root Mean Square Error (RMSE) of 12 m. A point marking device was used to drill 40 micrometer circular holes at the control points in the emulsion of the band 3 image. The control points then were transferred and drilled onto images of bands 1, 5, and 7 using binocular vision and the drilled holes on band 3 as the "master". Therefore, any errors arising during the transfer of the control points from the map to

ORIGINAL PAGE IS
OF POOR QUALITY

the band 3 image also are present in the other bands. Cartesian coordinates of each control point on each band then were measured by means of a photogrammetric comparator whose resolution is one micrometer.

Universal Transverse Mercator (UTM) projection coordinates for each of the control points were measured from the topographic maps and recorded to the nearest 5 m using a metric coordinate reader (a transparent plastic template). The UTM coordinates were transformed numerically to latitude-longitude and then to Space Oblique Mercator (SOM) coordinates.

The coefficients of two transformations, the similarity and the affine, were calculated by the least-squares method by using the measured comparator coordinates, and their respective UTM and SOM coordinates. The similarity transformation can be interpreted as a rotation, single change in scale and two translations:

$$\begin{aligned} x' &= ax + by + x_0 & a &= K \cos 0 \\ y' &= -bx + ay + y_0 & b &= K \sin 0 \end{aligned}$$

when K is the scale change, 0 is the rotation, and x_0 , y_0 are the translations.

The affine transformation is a six-parameter transformation permitting two mutually perpendicular scale changes, two rotations (one defining the direction of the scale changes), and two translations:

$$\begin{aligned} x' &= ax + by + x_0 \\ y' &= cx + dy + y_0 \end{aligned}$$

Table 1 shows the vector residuals resulting from each transformation for the four TM bands measured to date.

Table 1
ROOT MEAN SQUARE ERROR (RMSE) OF VECTOR RESIDUALS
FROM CONTROL MEASUREMENT

TM band	<u>UTM ground coordinates</u>		<u>SOM ground coordinates</u>	
	Similarity	Affine	Similarity	Affine
1	72 m	45 m	70 m	43 m
3	70 m	45 m	67 m	42 m
5	68 m	43 m	66 m	46 m
7	69 m	45 m	66 m	41 m

In all cases, the SOM projection fits the data slightly better, i.e. has a smaller RMSE, than the UTM projection, but little difference in shape exists between a scene recorded on film in either of the two map projections. The difference probably will be smallest for those areas in which the scene center coincides with a UTM central meridian; at these locations the higher order terms of the two projections are minimal.

ORIGINAL PAGE IS
OF POOR QUALITY

Table 1 shows that the application of the affine transformation significantly reduces the root mean square error in all cases. One possible cause may be the film-writing device. A highly significant skewness had been observed in 1980 from tests of grids printed from the same device as used in this study (N. Falcone, U.S. Geological Survey, personal communication). At that time, it was hypothesized that it possibly was caused by lack of parallelism between the axis of the rotary drum and the axis of travel of the light source. In order to verify the 1980 findings, a new six by six grid, having 4 cm spacing, was written on film using a 50 micrometer aperture. The RMSE values are given in Table 2 along with those of the 1980 measurements:

Table 2
ROOT MEAN SQUARE ERROR OF VECTOR RESIDUALS
FROM GRID MEASUREMENTS

	Similarity	Affine
1980 Grid	136 micrometers	75 micrometers
1983 Grid	117 micrometers	21 micrometers

Although the values for the 1983 grid are smaller, a significant affine error is still indicated. Vector plots of residuals from the similarity transformation display an extremely high degree of correlation between the two sets of grids. Figures 2 and 3 are vector plots of residuals for the 1983 grids. Figure 2 indicates a general elongation inclined at 45° to the direction of the lead screw which moves the light source and a compression at 90° to the prior direction. Figure 3 is a plot of residuals remaining after the removal of first order errors. One can surmise, from examination of the residuals, that at least a third order polynomial is necessary to reduce the residuals to the same order of magnitude as the measuring errors (approximately 3 micrometers).

In order to assess the difference in shape between the UTM and SOM map projections, their respective sets of coordinates of the control points were fit together by the least-squares method. The similarity transformation results in a RMSE of 11.3 m for the 38 control points, whereas the affine transformation results in a value of 11.4 m. Because both projections are conformal, it is not surprising that the affine transformation does not reduce the residuals.

Band-to-band registration was checked for the Washington, D.C. scene viewing several small parts of the scene on an interactive video display device. Several strongly contrasting targets, such as airport runways and small ponds, were used to visually determine the offsets. By rapidly toggling between the TM bands on the interactive system it was found that bands 1 through 4 were coregistered nearly perfectly (fig. 4a). Using channels 1 through 4 as references, bands 5 and 7 were found to be displaced 1 to 2 pixels westward (fig. 4b). Band 6 was displaced 4 pixels eastward (fig. 4c), which effectively means it is displaced by one of its 120 m resolution units.

RADIOMETRIC ANALYSIS

ORIGINAL PAGE IS
OF POOR QUALITY

A geometrically uncorrected version (GSFC A-tape digital format) of the Macon, Georgia scene was examined to determine some of the radiometric characteristics of the data. This included analysis of the 16 individual detectors in bands 1 through 5 and 7 and each of 4 detectors of channel 6. Systematic gaps were found within the limited range of digital numbers recorded for the scene. These can be attributed to the integer truncation of decimal numbers involved in the calibration procedure during production of the computer compatible tapes.

The potential of sensor striping caused by the separate gains and offsets required for each of the 16 sensors of the visible and near-infrared TM bands was investigated using the A-tape of the Macon scene. The four sensor thermal infrared band also was examined. Means and standard deviations were calculated on a modulo-16 basis. The results are summarized in table 3.

Table 3

COMPARISON OF DIGITAL NUMBER STATISTICS
FOR MODULO-16 STRIPING OF TM DATA

<u>TM Channel</u>	<u>1</u>	<u>2</u>	<u>3</u>	<u>4</u>	<u>5</u>	<u>6</u>	<u>7</u>
range of	85.5	34.2	30.6	74.5	66.8	126.0	22.7
sensor means	86.4	34.8	31.2	74.9	67.1	126.7	23.1
difference	0.9	0.6	0.5	0.4	0.3	0.7	0.4
range of							
standard	17.649	9.067	11.295	16.665	23.449	15.527	11.679
deviations	18.076	9.504	11.661	17.026	23.931	15.980	12.271
difference	0.427	0.437	0.366	0.361	0.482	0.453	0.592

The range of means is typically less than that of Landsat MSS values when the MSS data are scaled into 8-bit space. Enhanced-contrast images of parts of the Macon scene were recorded onto film and visually examined for evidence of striping. Striping is not evident in channels having sensors with a range of mean differences less than 0.4 between their high and low values. Striping becomes apparent when difference values reach 0.5 and becomes objectionable when values are greater than 0.6.

A banding also was noted for some of the TM bands over homogeneous targets such as water bodies. The banding appears clustered into two groups of 16 adjacent scanlines and appears to be related to the alternate back and forth sweeps of the pushbroom scanner.

P-tape data for the Florida scene were analyzed to assess the radiometric character of the banding. Because the data have been geometrically corrected and interpolated to a 28.5 m pixel size, the gathering of banding statistics was done on groups of 17 scanlines, which is an approximation to the required correction of a 30 m original pixel to the geometrically corrected pixel size

ORIGINAL PAGE IS
OF POOR QUALITY

of 28.5 m. The relationship should hold for at least a small contiguous group of scanlines. Two areas along the same groups of 17 scanlines were sampled over relatively homogeneous bodies of water. Statistics were contrasted for waters of Lake Weir, Florida, on the western side of the image, against the Atlantic Ocean waters located off Edgewater, Florida, near the east edge of the image (Tables 4 and 5).

TABLE 4

COMPARISON OF DIGITAL NUMBER STATISTICS, TWO HOMOGENEOUS
WATER BODIES ALONG THE SAME, BUT OPPOSITE ENDS OF GROUPS OF
17 SCANLINES

Lake water

Scanlines	TM Band	1	2	3	4	5	6	7
2809-2825	Mean	78.97	29.07	23.01	17.22	9.41	131.51	4.24
	Std. Dev.	1.44	0.63	0.66	0.47	0.68	0.50	1.08
2826-2842	Mean	79.92	29.33	23.34	17.36	9.41	131.68	4.27
	Std. Dev.	1.46	0.61	0.73	0.49	0.78	0.47	0.96
2843-2859	Mean	78.74	29.00	23.00	17.15	9.36	131.68	4.31
	Std. Dev.	1.42	0.68	0.70	0.43	0.79	0.47	1.05
2860-2876	Mean	79.24	29.13	23.22	17.37	9.40	131.72	4.28
	Std. Dev.	1.54	0.68	0.74	0.52	0.79	1.45	1.04
2877-2893	Mean	78.57	28.82	22.99	17.07	9.38	131.71	4.31
	Std. Dev.	1.60	0.69	0.72	0.45	.74	0.46	1.04

Sample size for each group of scanlines = 272

TABLE 5

COMPARISON OF DIGITAL NUMBER STATISTICS, TWO HOMOGENEOUS
WATER BODIES ALONG THE SAME, BUT OPPOSITE ENDS OF GROUPS OF
17 SCANLINES

Ocean water

Scanlines	TM Band	1	2	3	4	5	6	7
2809-2825	Mean	74.71	25.26	19.39	12.25	6.91	129.44	3.89
	Std. Dev.	1.42	0.69	0.68	0.66	0.92	0.61	1.01
2826-2842	Mean	73.44	24.78	18.83	11.03	6.84	128.39	3.82
	Std. Dev.	1.36	0.60	0.68	0.69	0.98	1.63	1.02
2843-2859	Mean	74.53	25.40	19.40	12.31	6.82	129.44	3.87
	Std. Dev.	1.31	0.69	0.72	0.75	0.92	0.67	1.04
2860-2876	Mean	73.49	24.95	18.94	11.16	6.89	129.17	3.85
	Std. Dev.	1.24	0.72	0.68	0.69	1.01	0.49	0.97
2877-2893	Mean	74.98	25.61	19.61	12.50	6.83	129.47	3.92
	Std. Dev.	1.48	0.63	0.71	0.68	0.95	0.70	1.05

Sample size for each group of scanlines = 272

ORIGINAL PAGE IS
OF POOR QUALITY

Both these areas exhibited banding in the image data. The beginning of the groups of 17 scanlines was determined by using a harshly contrast-enhanced TM band 3 image and picking the beginning scanline on an interactive video analysis system. Examination of table 5 shows that the ocean waters have a consistent variation in mean values for groups of 17 adjacent scanlines, beginning with all channels having high mean values for the first group of 17 lines (2809-2825), and proceeding in an alternating low-high fashion for following groups of 17 lines. Digital values for the lake waters (table 4) show an opposite trend. The same initial group of scanlines shows consistently low values and proceeds in an alternating high-low fashion for following groups of 17 scanlines. Differences between adjacent groups of scanlines are greatest in TM channels 1 through 4, and appear negligible in TM band 5-7. The change in relative mean values across the image for adjacent groups of scanlines suggests an inherent and systematic change occurring, perhaps due to some decay factor imposed on the gain or offset values for opposite sweeps of the pushbroom scanner. Some crossover point must exist in the data, presumably near the center of the scanline, where digital numbers for opposite sweeps would be of equal value. It also suggests that this type of banding could not be corrected by a modulo-16 or -32 histogram equalization, even in the geometrically uncorrected A-tape data, unless correction factors which varied as a function of position along a scanline, were applied along groups of 32 scanlines.

PRELIMINARY SPECTRAL OBSERVATIONS

Specific band ratios were used to determine their effectiveness in defining vegetation and rock mineralogy for the Washington, D.C. scene. The TM 3/4 band ratio was selected to depict vegetation. Vegetation appears black to dark gray in this ratio because of its relatively low reflectance in band 3 due to the presence of chlorophyll absorption bands, and its high reflectance in band 4 due to a lack of chlorophyll absorption (Knipling, 1970). Geologic materials lack the strong contrast between TM bands 3 and 4 and thus would appear light gray to white in the ratio. The 5/2 band ratio was used to depict limonitic rocks. Limonitic rocks have low reflectances in bands 1 and 2 compared with band 3 due to a strong ferric-iron absorption band centered in the ultraviolet, but whose effects reach into the short wavelength visible part of the spectrum (Hunt and others, 1971; Hunt and Ashley, 1979). Nonlimonitic rocks and soils lack the absorption band in the ultraviolet, hence their spectral curves do not show the sharp drop between band 3 and bands 1 and 2. Most geologic materials have no absorption bands in TM band 5 and are quite bright in this region of the spectrum. Hence, a 5/2 band ratio image will appear relatively bright for limonitic rocks, whereas nonlimonitic rocks will appear dark.

Rocks which have minerals that contain hydroxyl or carbonate anions in their crystal lattices, have absorption bands (Hunt and Salisbury, 1971; Hunt and Ashley, 1979) in the bandpass of TM band 7. Hydroxyl-bearing minerals, those containing either Al-O-H or Mg-O-H bands, include: 1) clay minerals, 2) other sheet silicates such as the serpentine minerals, some of the micas, and talc, among others, and 3) sulfate minerals such as alunite and jarosite, which often are found as products of hydrothermal alteration processes. Carbonate minerals include calcite and dolomite, which are common constituents in the

sedimentary rocks limestone and dolomite. Rocks containing these anions will have relatively low reflectance values in TM band 7, whereas rocks lacking these anions will have relatively higher reflectances. A 5/7 band ratio was evaluated to test the effectiveness of the 1.6- and 2.2-um bands in detecting rocks containing hydroxyl- or carbonate-bearing minerals. Areas containing rocks which have absorption bands in the 2.2-um region will appear light gray to white in the 5/7 ratio, whereas rocks lacking absorption bands in this region will appear dark gray to black. Similar bands were selected in prior studies to map clay-rich rocks using airborne Thematic Mapper Simulator (TMS) scanners (Podwysocki and Segal, in press; Rowan and Kahle, 1982; Ashley and Abrams, 1980). Preliminary results show that clay minerals containing absorption bands at 2.2 um, which are centered in TM band 7, can be readily detected when the band ratio images are suitably contrast-enhanced.

Figure 5a is a false-color infrared image which shows a 256 by 256 pixel area from the Washington, D.C. scene. A road construction project has laid bare clay-rich soils containing ferric iron oxide minerals. A color ratio composite image (fig. 5b) shows the clear barren area as white, which in the color assignments made to each ratio, indicates both ferric iron oxide and clay minerals. Ferric-iron-rich areas lacking clay minerals are portrayed as a cyan color. Vegetation appears red to magenta, depending upon its type and vigor. Spectrally flat areas (lacking both ferric iron and clay absorption bands) are green to yellow-green.

SUMMARY

Landsat-4 Thematic Mapper digital data were examined for several scenes in the eastern United States to characterize their geometric and radiometric accuracies. A small portion of one of the scenes also was processed using band ratioing in order to test the radiometric characteristics for mapping of spectrally dissimilar geologic materials.

Whole-scene accuracy was assessed by comparison of 38 image and topographic control points for four bands of a TM image of the Washington, D.C. area. The images were compared with both Universal Transverse Mercator and Space Oblique Mercator projections. Both similarity and affine transformations were applied using the least-squares method in order to fit the image control points to the map coordinates. Results show that the affine transformation provides a better fit of the image to the map projections, decreasing the root mean square error from an average of about 70 m for the similarity transformation to about 45 m for the affine transformation for both projections. Results show that little difference exists between the two projections for this TM scene. Analysis of the geometry of the film-writing device that was used to produce the TM images suggests a systematic error in the device, causing an elongation along one diagonal of the image and a foreshortening along the opposite diagonal. This distortion in the film-writer device accounts for most residual error found in the similarity transformation of the TM image data. Hence, geometric errors in the TM data itself, are of some value less than or equal to the RMSE values derived from the affine transformation.

Band-to-band registration for portions of the Washington, D.C. scene indicates subpixel misregistration in TM bands 1 through 4. TM bands 5 and 7 are displaced between 1 to 2 pixels from their corresponding points in the bands 1 through 4 and band 6 is displaced by 3 to 4 pixels from bands 1 through 4.

Analysis of the radiometric quality shows at least two types of scanline-related banding. Radiometric stripping occurs on a modulo-16 basis and is related to small shifts in gains and/or bias between each of the 16 detectors in each band. Stripping is most noticeable in band 1 and becomes less noticeable with increasing wavelength in the visible and near-infrared bands. The thermal band six also has relatively pronounced banding. Another type of banding appears as alternating groups of 16 lighter and darker scanlines. The effect is noticed over homogenous areas such as water bodies and is most pronounced along the edges of the scenes. The effect changes along the length of the groups of 16 scanlines. Along one edge of the scene, average values of the 16 scanlines alternate in a high-low fashion, whereas on the opposite side of the scene, values alternate in a low-high fashion for the same scanlines. The severity of the banding is worse in band 1 and becomes less and less noticeable towards the near infrared. TM band 6 is not affected by the phenomenon.

TM bands were ratioed in order to test the radiometric quality of the data for mapping geologic units with contrasting spectral characteristics. A 3/4 band ratio was processed to distinguish between vegetation and other materials. A 5/2 ratio was used to distinguish between limonitic and nonlimonitic rocks and a 5/7 ratio was used to detect geologic materials which contained minerals having the hydroxyl or carbonate anion. Results showed that clay and limonite-rich rocks could be distinguished from limonitic rocks lacking clays. Rocks lacking both limonite and clays could also be distinguished.

REFERENCES

Ashley, R. P., and Abrams, M. J., 1980, Alteration mapping using multispectral images - Cuprite mining district, Esmeralda County, Nevada: U.S. Geological Survey Open-File Report 80-367, 17p.

Bender, L.U. and Falcone N. 1982, Landsat 3 RBV Imagery for Topographic Mapping: Proceedings, Fifth International Symposium on Computer-Assisted Cartography and ISP Commission IV; Cartographic and Data Band Application of Photogrammetry and Remote Sensing, p. 45-54.

Hunt, G. R., and Salisbury, J. W., 1971, Visible and near-infrared spectra of minerals and rocks: II-Carbonates: Modern Geology, v. 2, p. 22-30.

Hunt, G. R., and Ashley, R. P., 1979, Spectra of altered rocks in the visible and near infrared: Economic Geology, v. 74, p. 1612-1629.

Hunt, G. R., Salisbury, J. W., and Lenhoff, D. J., 1971, Visible and near-infrared spectra of minerals and rocks: III-Oxides and hydroxides: Modern Geology, v. 2, p. 195-205.

Knipling, E. B., 1970, Physical and physiological basis for the reflectance of visible and near-infrared radiation from vegetation: Remote Sensing of the Environment, v. 1, no. 3, p. 155-159.

Podwysocki, M.H., and Segal, D.B., 1983, Mapping of hydrothermally altered rocks using airborne multispectral scanner data, Marysvale, Utah mining district: Economic Geology, v. 78, p. 675-687.

Rowan, L.C., and Kahle, A.B. 1982, Evaluation of 0.46- to 2.36-um multispectral scanner images of the East Tintic mining district, Utah, for mapping hydrothermally altered rocks: Economic Geology, v. 77, p. 441-452.

ORIGINAL PAGE IS
OF POOR QUALITY

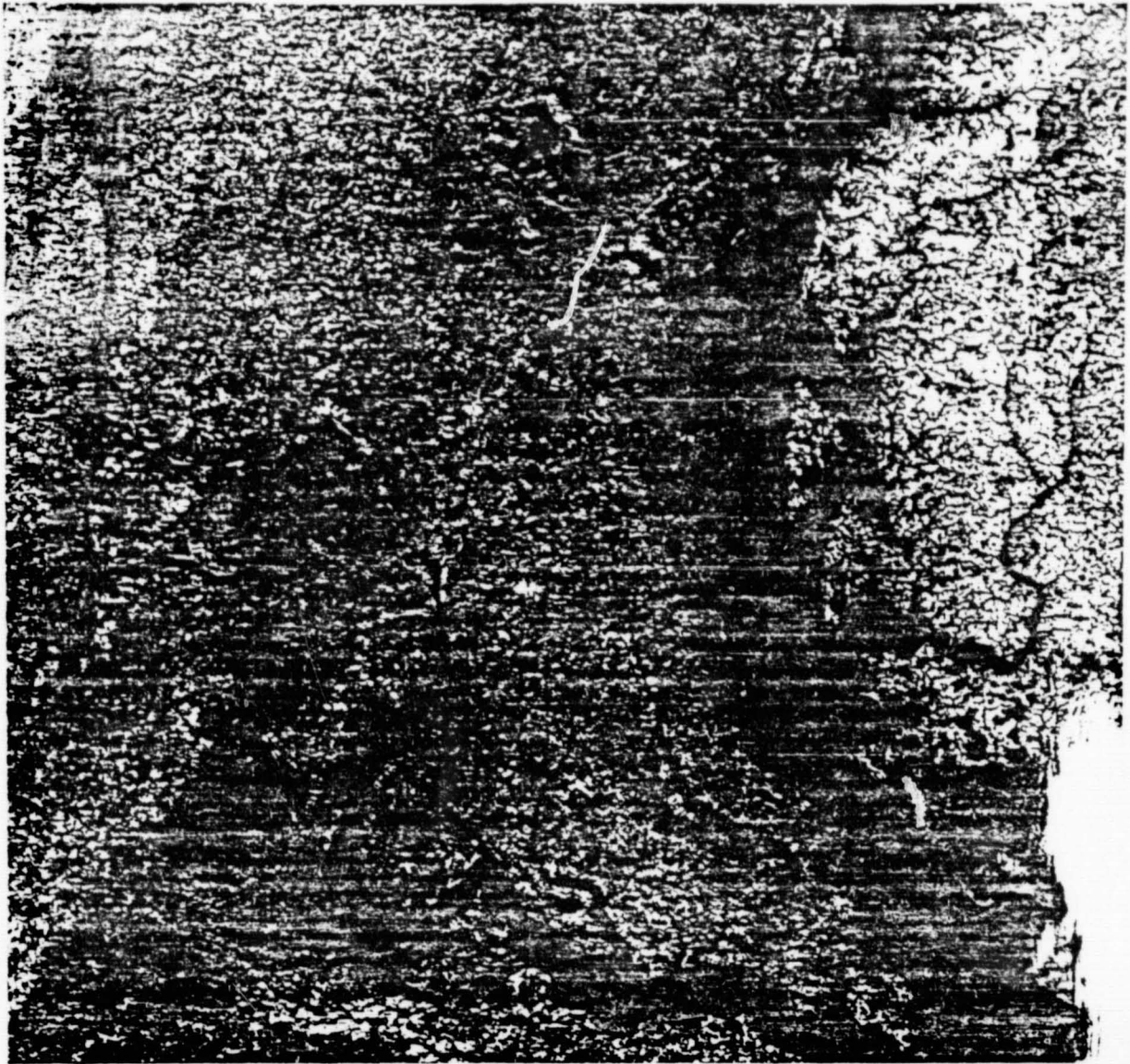


Figure 1a - Image of TM band 3 for the whole Washington, D.C. scene. Distance along the edge of the image is approximately 185 km.

ORIGINAL PAGE IS
OF POOR QUALITY

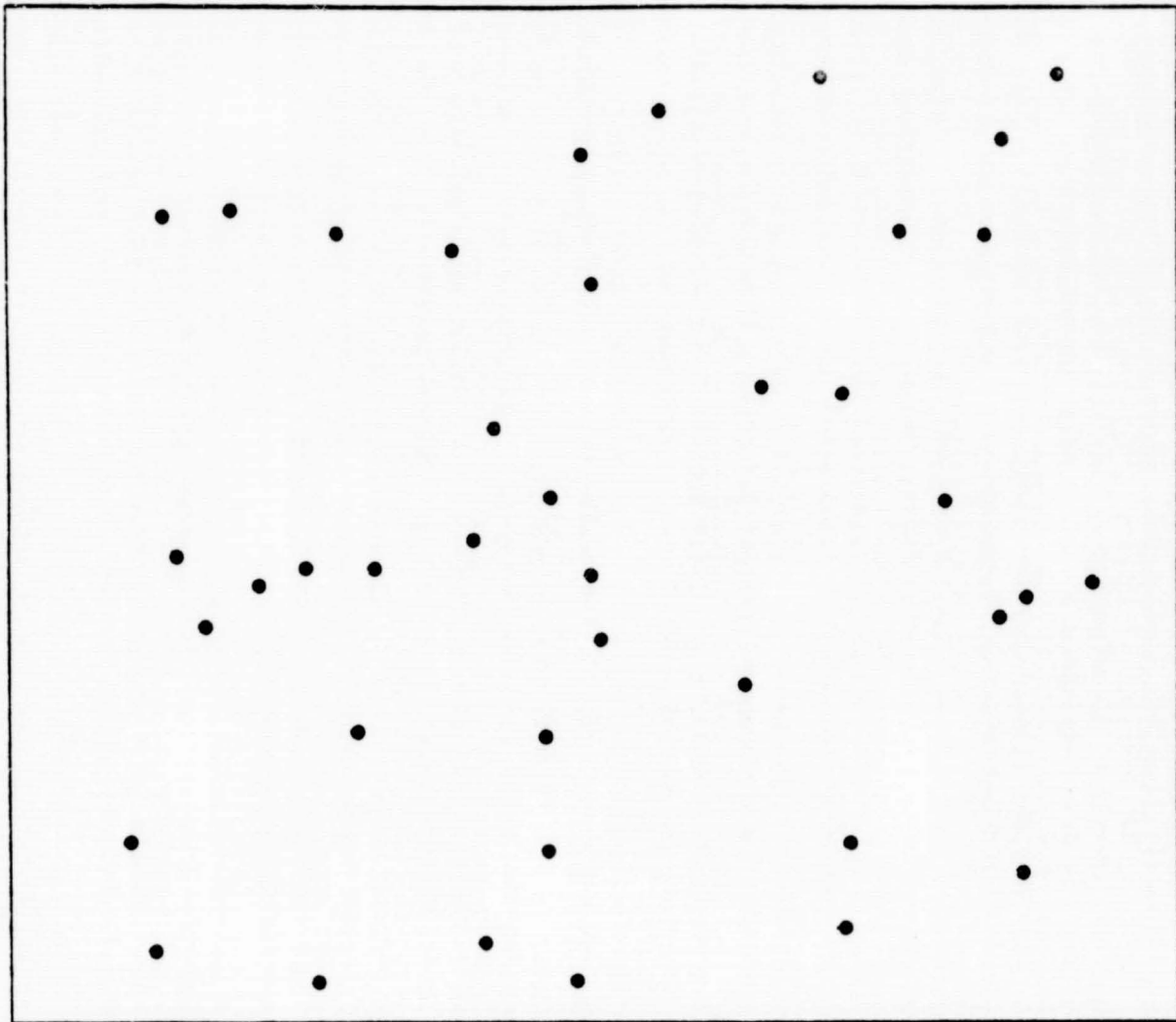


Figure 1b - Schematic map showing the distribution of 38 control points chosen for this study.

ORIGINAL PAGE IS
OF POOR QUALITY

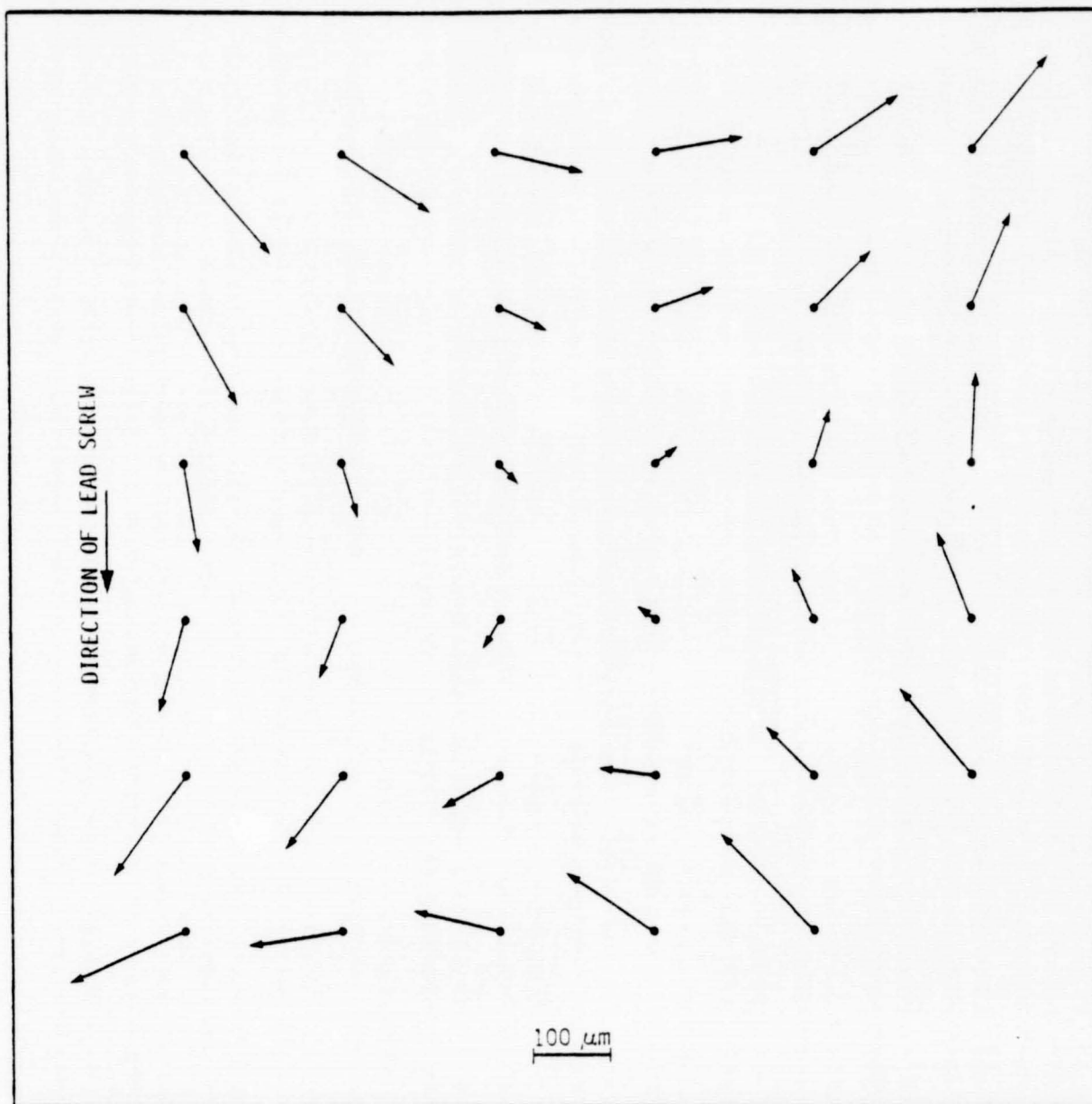


Figure 2 - A plot of residual errors resulting from application of the similarity transformation to the 4 cm-spaced grid data.

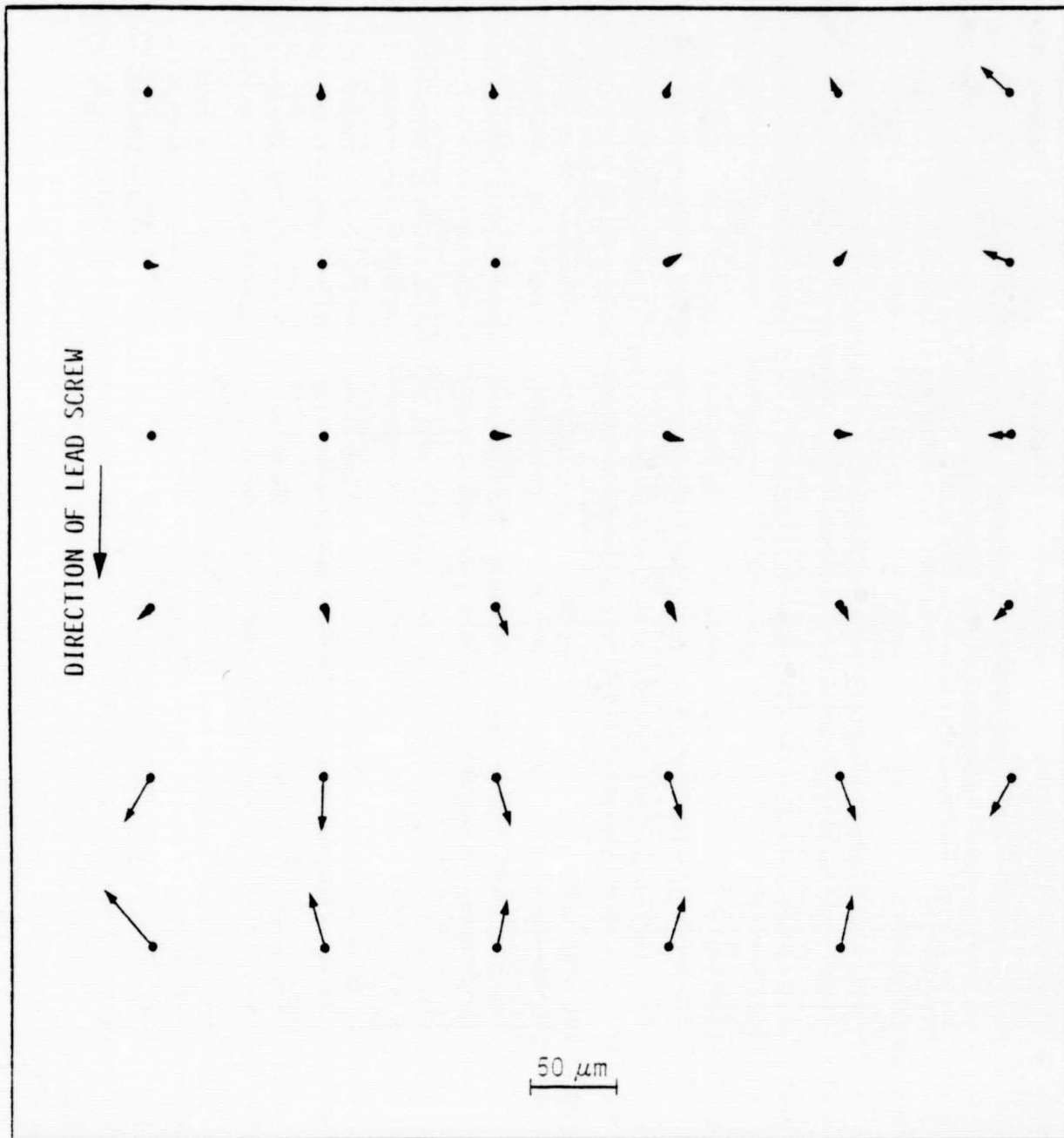


Figure 3 - A plot of residual errors resulting from the application of the affine transformation to the 4 cm-spaced grid data.

ORIGINAL PAGE IS
OF POOR QUALITY

Figures 4 - Color-composite images (64 by 64 pixels) of TM bands projected on the CRT as red, green, and blue, respectively, for a portion of Dulles International Airport. The runways and small lake were used to study band-to-band registration. Distance along bottom edge of the image is approximately 1.8 km.

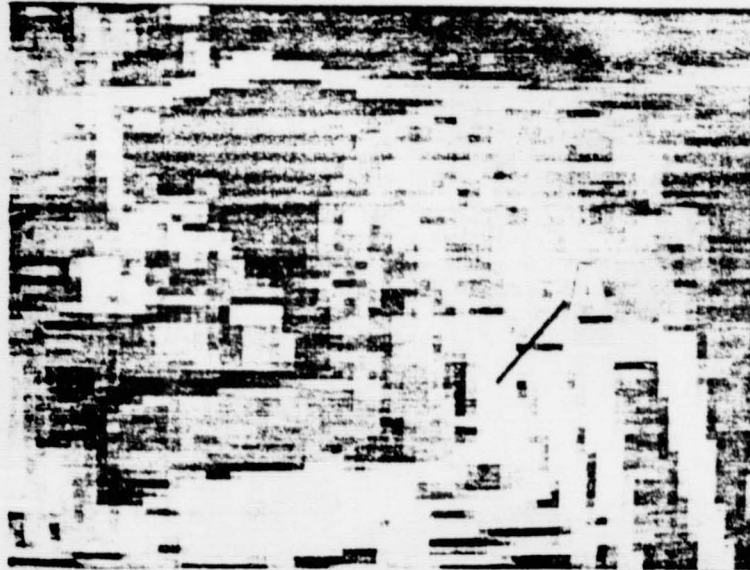


Figure 4a - A composite image of bands 4, 3, and 2. Misregister appears to be at the subpixel level. Note that the brightest portion of the airport parking ramp (A) is centered in the middle of the ramp (cf. fig. 4b).



Figure 4b - A color-composite of bands 5, 3, and 2. Note that the brightest portion of the airport parking ramp (A) is shifted, indicating a westward shift of approximately one pixel for band 5.

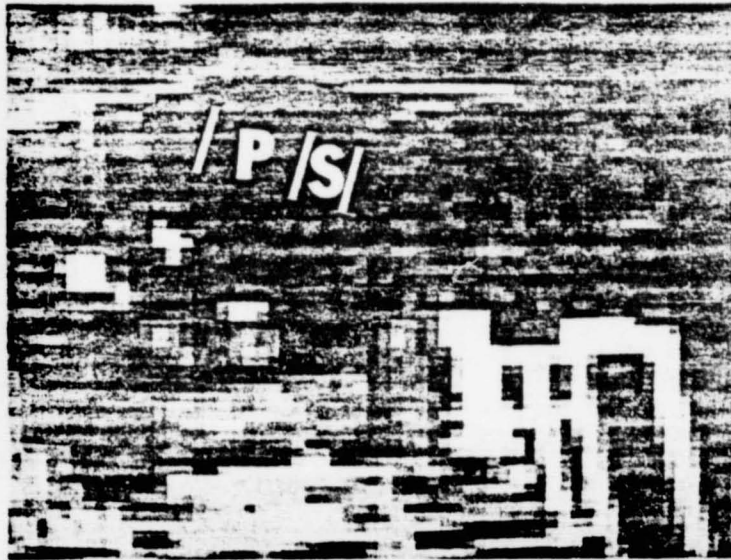


Figure 4c - A composite of bands 6, 3, and 2. The pond (P) appears shifted 4 pixels east in band 6, as noted by the dark "shadow" east of the pond.

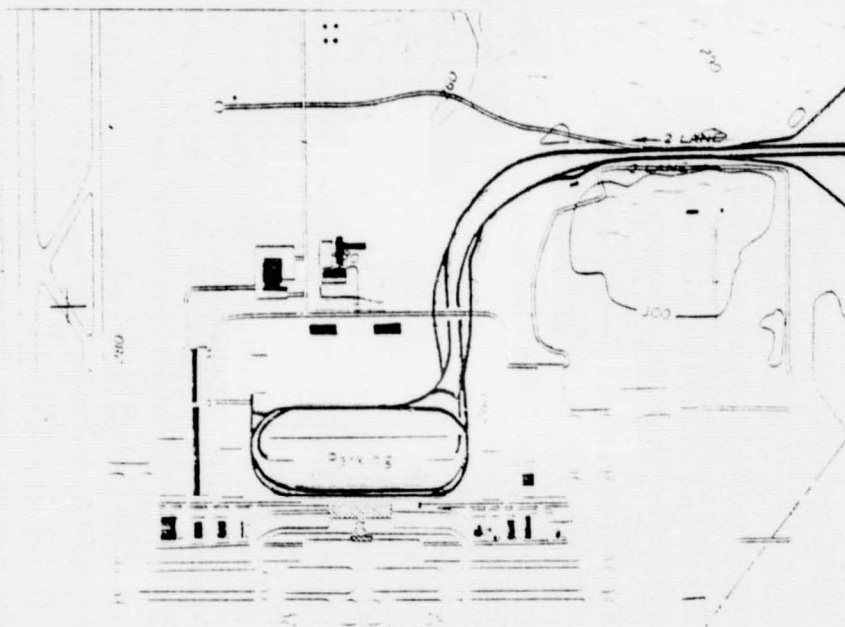


Figure 4d - Topographic map of Dulles International Airport.

SCALE 1:24 000

ORIGINAL PAGE IS
OF POOR QUALITY



Figure 5a - A TM false-color infrared composite of bands 4, 3 and 2 projected as red, green, and blue, respectively. The bright white linear area in the northeast quadrant (C) is an area of disturbed ground along a highway right-of-way containing clay-rich limonitic soils. Distance across the bottom edge of the image is approximately 7.3 km.

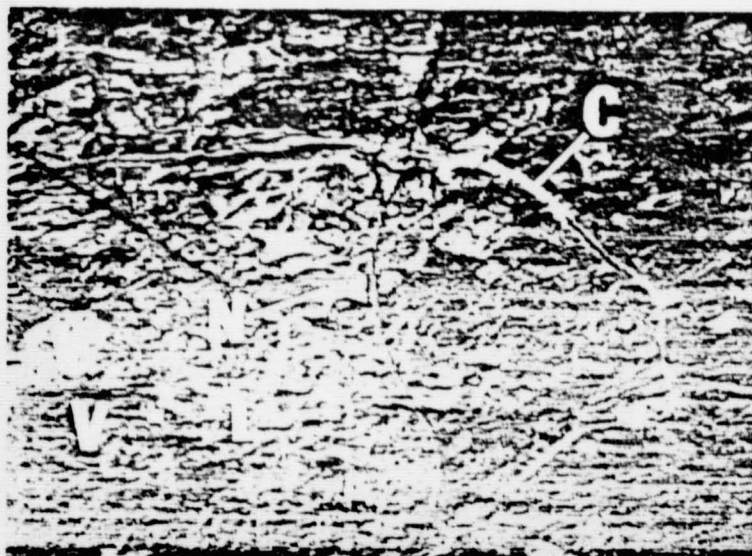


Figure 5b - A color-ratio-composite image of TM band ratios 3/4, 5/2 and 5/7 projected as green, blue and red, respectively. Areas of limonitic material (L) appear cyan, limonitic and clay-rich areas are white (C) bare areas containing neither limonite nor clay minerals are yellow-green to green (B). Vegetation appears in shades of red to magenta (V).

ORIGINAL PAGE IS
OF POOR QUALITY

Figures 4 - Color-composite images (64 by 64 pixels) of TM bands projected on the CRT as red, green, and blue, respectively, for a portion of Dulles International Airport. The runways and small lake were used to study band-to-band registration. Distance along bottom edge of the image is approximately 1.8 km.

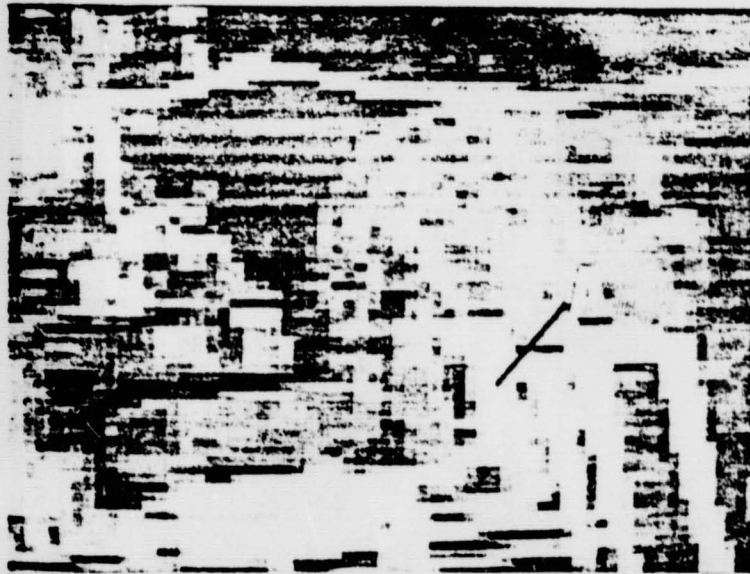


Figure 4a - A composite image of bands 4, 3, and 2. Misregister appears to be at the subpixel level. Note that the brightest portion of the airport parking ramp (A) is centered in the middle of the ramp (cf. fig. 4b).

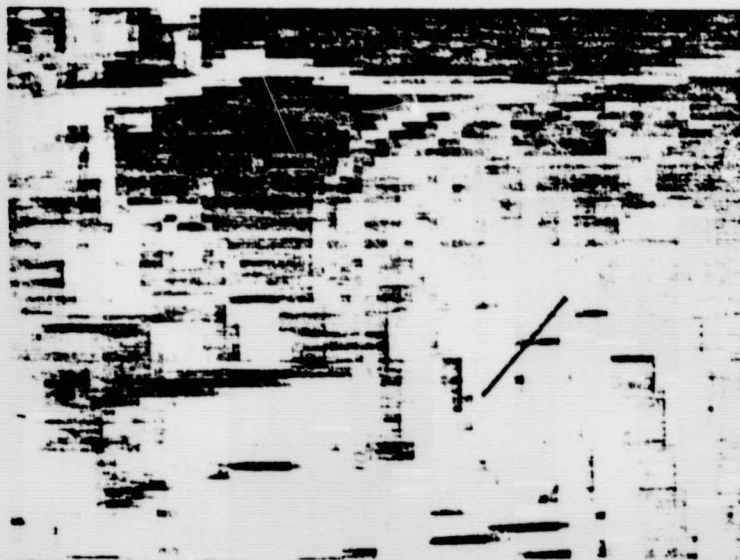


Figure 4b - A color-composite of bands 5, 3, and 1. Note that the brightest portion of the airport parking ramp (A) is shifted, indicating a westward shift of approximately one pixel for band 5.

ORIGINAL PAGE IS
OF POOR QUALITY



Figure 5a - A TM false-color infrared composite of bands 4, 3 and 2 projected as red, green, and blue, respectively. The bright white linear area in the northeast quadrant (C) is an area of disturbed ground along a highway right-of-way containing clay-rich limonitic soils. Distance across the bottom edge of the image is approximately 7.3 km.



Figure 5b - A color-ratio-composite image of TM band ratios 3/4, 5/2 and 5/7 projected as green, blue and red, respectively. Areas of limonitic material (L) appear cyan, limonitic and clay-rich areas are white (C) bare areas containing neither limonite nor clay minerals are yellow-green to green (W). Vegetation appears in shades of red to magenta (V).